CLINICAL ORTHOPAEDICS AND RELATED RESEARCH
Number 458, pp. 117–124

Range of Motion in Anterior Femoroacetabular Impingement

M. Kubiak-Langer, MSc[*]; Moritz Tannast, MD[†,‡]; S. B. Murphy, MD[‡]; K. A. Siebenrock, MD[†]; and F. Langlotz, PhD[*]

The range of motion of normal hips and hips with femoroacetabular impingement relative to some specific anatomic reference landmarks is unknown. We therefore described: (1) the range of motion pattern relative to landmarks; (2) the location of the impingement zones in normal and impinging hips; and (3) the influence of surgical débridement on the range of motion. We used a previously developed and validated noninvasive 3-D CT-based method for kinematic hip analysis to compare the range of motion pattern, the location of impingement, and the effect of virtual surgical reconstruction in 28 hips with anterior femoroacetabular impingement and a control group of 33 normal hips. Hips with femoroacetabular impingement had decreased flexion, internal rotation, and abduction. Internal rotation decreased with increasing flexion and adduction. The calculated impingement zones were localized in the anterosuperior quadrant of the acetabulum and were similar in the two groups and in impingement subgroups. The average improvement of internal rotation was 5.4° for pincer hips, 8.5° for cam hips, and 15.7° for mixed impingement. This method helps the surgeon quantify the severity of impingement and choose the appropriate treatment option; it provides a basis for future image-guided surgical reconstruction in femoroacetabular impingement with less invasive techniques.

Received: June 16, 2006
Revised: September 22, 2006
Accepted: December 15, 2006
From the [*]MEM Research Center for Orthopaedic Surgery, Institute for Surgical Technology and Biomechanics, University of Bern, Bern, Switzerland; the [†]Department of Orthopaedic Surgery, Inselspital, University of Bern, Bern, Switzerland; and the [‡]Center for Computer Assisted and Reconstructive Surgery, New England Baptist Hospital, Tufts University, Harvard Medical School, Boston, MA.
One or more of the authors (MT, SBM, KAS, FL) has received funding from the National Center for Competence in Research "Computer Aided and Image Guided Medical Interventions (Co-Me)," a fellowship for prospective researchers of the Swiss National Science Foundation (SNF), a Travel Fellowship Award from the International Society for Computer Assisted Orthopaedic Surgery (CAOS International), and the 2005 Research Grant Award from the New England Baptist Hospital.
Each author certifies that his or her institution has approved the human protocol for this investigation, that all investigations were conducted in conformity with ethical principles of research, and that informed consent for participation in the study was obtained.
Correspondence to: Moritz Tannast, MD, Department of Orthopaedic Surgery, Inselspital, University of Bern, Murtenstrasse, 3010 Bern, Switzerland. Phone: 41-31-632-2222; Fax: 41-31-632-3600; E-mail: moritz.tannast@insel.ch.
DOI: 10.1097/BLO.0b013e318031c595

The human hip is a ball and socket type of joint with three degrees of freedom. Any loss of clearance between the femoral neck and acetabular rim compromises hip excursion. As a clinically concomitant of this concept, femoroacetabular impingement occurs when bony prominences of the femoral head–neck junction (cam impingement) and/or the acetabular rim (pincer impingement) lead to early contact, causing substantial labral and prearthrotic chondral damage, particularly in young and active adults.[5,6,9,16,19,20]

Based on routine clinical examinations, several previous studies report patients with femoroacetabular impingement typically have restricted flexion, internal rotation, and abduction.[9,13,19] However, substantial errors in clinical measurements can occur if the examiner fails to recognize individual tilt or pelvic rotation. Tilt and rotation are difficult to know or control during an examination and can vary considerably when the patient is in the supine position.[7,22] A better preoperative assessment of impingement-free motion and identification of impingement location may help the surgeon's decision-making process for ascertaining appropriate operative treatment. A complete surgical dislocation to observe the pathomechanism[12] is unnecessary if the impingement source can be detected accurately preoperatively. In addition, if the exact amount of bone to be resected is known preoperatively, less invasive approaches (eg, arthroscopy) can be performed with higher precision for surgical treatment of femoroacetabular impingement.

We used previously developed and validated software for kinematic hip simulation to quantify surgically simulated femoroacetabular osteoplasty to address three questions: (1) What is the range of motion pattern for assessing femoroacetabular impingement in impinging hips com-

pared with normal hips; (2) where is the impingement zone in hips with anterior femoroacetabular impingement in comparison to normal hips; and (3) does the range of motion pattern change after virtual quantified surgical treatment for femoroacetabular impingement? We hypothesized: (1) hips with anterior femoroacetabular impingement would have decreased internal rotation for all possible combinations of flexion and abduction/adduction; (2) the impingement zones would be localized in the anterosuperior part of the acetabulum; and (3) internal rotation would increase after virtual surgical débridement for femoroacetabular impingement.

MATERIALS AND METHODS

We created a virtual 3-D model of the hip using CT scans acquired with a standard helical scanner. We then analyzed individual hip motion patterns to simulate quantifiable surgical treatment for femoroacetabular impingement abnormalities. The CT scan has to cover the pelvis and the proximal and distal parts of the femur, including the epicondylar area (Fig 1). We used this volumetric data and a semiautomated intensity thresholding technique to create a virtual 3-D model of the patient's hip.

We used two anatomic coordinate systems (one for the pelvis and one for the femur) to define neutral hip orientation (Fig 1). The anterior pelvic plane representing the pelvic coordinate system was constructed by both anterior superior iliac spines and the two pubic tubercles.[4,22] The femoral coordinate system by Murphy et al used the posterior aspects of the two femoral condyles, the knee center, and the center of the femoral head.[15] The virtual 3-D model of the patient's hip and the three 2-D cross-sectional views were used to locate these anatomic landmarks. To facilitate accurate position of the rotation center, a virtual circle was fitted to the contour of the femoral head in the three 2-D cross-sectional views by translating the center of the circle or by changing its radius. The concavity of the anterior femoral head–neck junction was quantified by the alpha angle formed between the axis of the femoral neck and the line connecting the center of the femoral head with the point of beginning asphericity according to the measurements of Nötzli et al.[17]

We applied a previously developed collision detection algorithm[8] to the volumetric hip data to compute a comprehensive range of motion (ROM) analysis with respect to the anatomic coordinate systems. To exclude undesirable artifacts-related impingement in the acetabular socket area affecting the simulation, the 3-D contour of the acetabular rim was manually defined. In addition to the recommended hip motions according to the guidelines of the American Academy of Orthopaedic Surgeons[7] (flexion/extension, abduction/adduction, internal/external rotation, and internal/external rotation in 90° flexion), the software allows motion patterns for any triaxial combination based on the previously introduced anatomic coordination systems (Fig 2). The ROM and location of impingement can be animated for any pattern.

Two processing modes are possible to provide additional information about the extension of the individual femoral and acetabular impingement zones. The first mode performs a predefined combined flexion and internal rotation mimicking the impingement pain test.[6] The second requires the user to define the maximum values for any simulated motion direction. The set

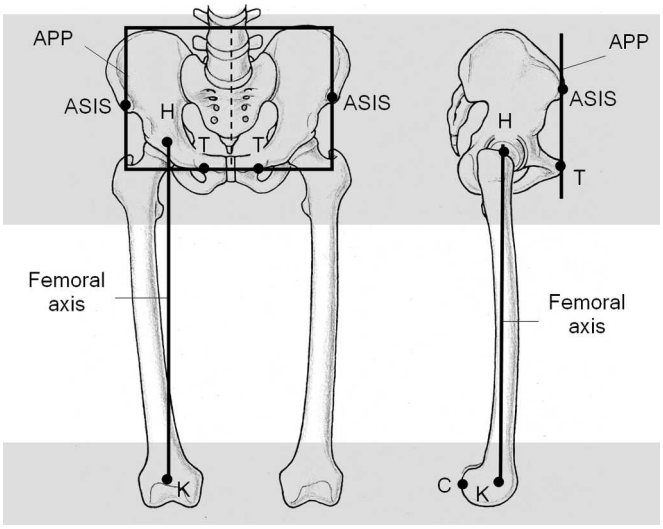

Fig 1. The definition of neutral orientation and visualization of the reference coordinate systems for the pelvis and femur is shown. The pelvic reference is the anterior pelvic plane defined by both anterior superior iliac spines (ASIS) and the midpoint of the pubic tubercles (T). The femoral axis runs through the hip (H) and the knee center (K) with the intercondylar line (C) lying parallel to the anterior pelvic plane. The CT scan has to cover the pelvis and the proximal and distal parts of the femur, including the epicondylar area (hatched area).

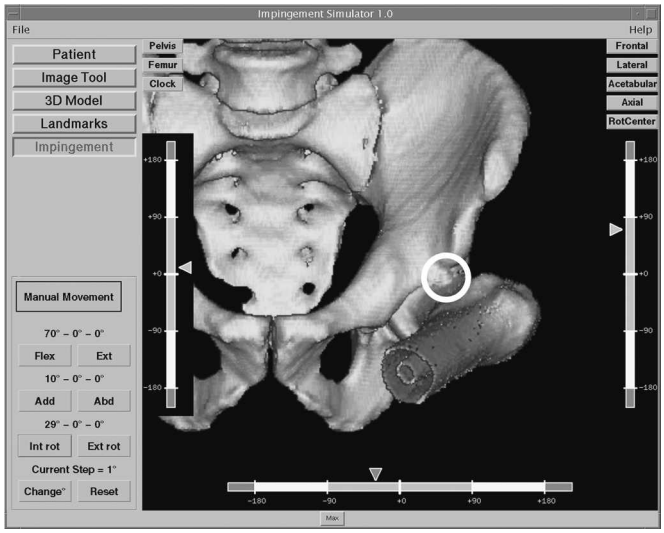

Fig 2. A screenshot of the developed software shows the 3-D reconstruction of a patient's hip and the impingement point (green dot or white circle, respectively) in the current orientation of 70° flexion, 10° adduction, and 29° internal rotation.

of resulting impingement zones can be displayed on the acetabular rim and quantified according to a previously described clockwise manner (Fig 3).[19] Stepwise manual adjustments of the joint motion with simulation of potential impingement zones are also available.

Quantified surgical acetabular and femoral osteoplasties were simulated according to current surgical practice.[12] Based on the extension of the acetabular impingement zone on the clock system, the acetabular segment to be trimmed was quantified with the maximum of resected rim depth in millimeters (Fig 3, distance x). Femoral offset creation was quantified with millimeter stepwise removal of the nonspherical portion of the femoral head–neck junction (distance y) with consecutive calculation of the resulting alpha angle (Fig 3). Distances x and y were chosen as parameters because they potentially can be used intraoperatively to transfer the preoperative computer plan to the operating room. The angle alpha, in contrast, cannot be measured directly intraoperatively.

Using the new volumetric data, automatic simulation of the improved ROM of the reconstructed hip was repeated. The results were provided in written form to enable the surgeon to judge whether correction on the acetabular side was adequate or needed additional modification.

After local Institutional Review Board approval, we then investigated differences in the ROM patterns between a consecutive series of hips with anterior femoroacetabular impingement (study group) and a cohort of normal hips (control group). All patients in the control group were recruited consecutively from patients treated at an outpatient clinic by one of the authors (SBM). A diagnosis of hip impingement was based on the current recommendations of a positive correlation among symptoms, physical findings (particularly a positive impingement test[6]), and suggestive 2-D radiographs. The normal group was selected from the contralateral hips of 146 patients undergoing CT-based, computer-assisted, image-guided THA. There were 33 normal hips and 28 hips with anterior femoroacetabular impingement (10 with cam type impingement, eight with pincer impingement, and 10 with mixed abnormalities). The mean patient age for the study group (35.4 ± 10.4 years; range, 19–49 years) was lower ($p < 0.0001$) in comparison to the control group (53 ± 11.1 years; range, 25–74 years). There were more ($p < 0.05$) men in the femoroacetabular impingement group (24 men, four women) than the control group (20 men, 13 women).

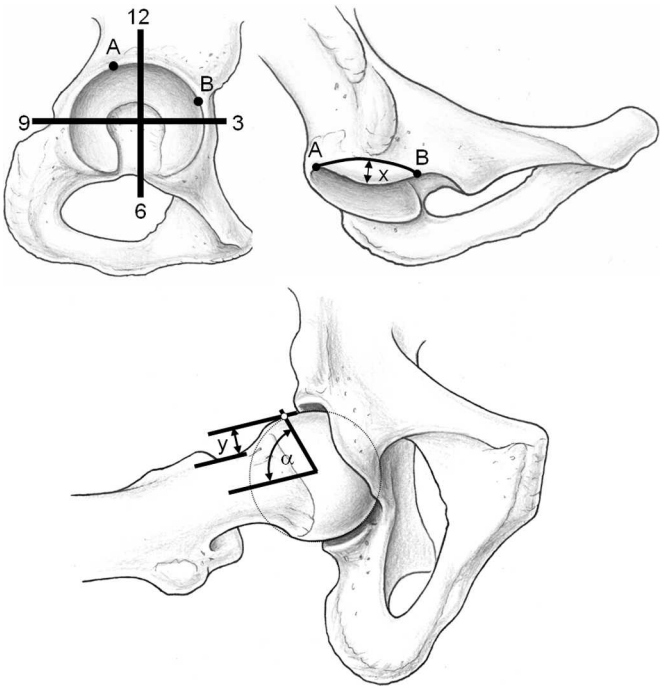

Fig 3. The acetabular segment to be trimmed (top) is quantified with an overlying clock system (A: beginning, B: end point) and the maximum depth of the segment in millimeters (x), which also can be reproduced intraoperatively. The femoral offset creation (bottom) is quantified with millimeter stepwise removal of the nonspherical portion of the femoral head-neck junction (y) with consecutive calculation of the resulting alpha angle.

We distinguished three subgroups in the femoroacetabular impingement group according to the cause of impingement: the pincer, the cam, and the combined subgroup. The pincer subgroup as the acetabular origin included hips with local or general overcoverage. Local overcoverage was defined by acetabular retroversion on conventional pelvic radiographs. General overcoverage comprised hips with radiographic evidence of coxa profunda or protrusio acetabuli. The cam subgroup included hips with an aspheric part of the femoral head–neck junction either in the lateral part of the femoral head (pistol grip deformity) or in the anterosuperior part of the femoral head–neck junction.

Based on a questionnaire and an anteroposterior pelvic radiograph, we formulated specific exclusion criteria for the control group to exclude hips with morphologic deformities such as dysplasia or femoroacetabular impingement, osteoarthritis, or patients with hip pain (Table 1). Because there was no axial radiograph for the uninvolved hip available, the anterior femoral head–neck offset was measured on the 3-D reconstructed hip according to Nötzli et al.[17]

A previous study showed a mean accuracy of –0.7° in angle detection of the developed computer program when used on sawbones.[21] In cadaver measurements, the software overestimates the real ROM by 5°.[21] There was high intraobserver and

TABLE 1. Exclusion Criteria for the Control Group

Category	Specific Criteria
Medical history	Total hip arthroplasty
	Pain
	Previous hip surgery
Conventional radiographic criteria	Grade 1 osteoarthritis or higher
	Lateral center edge (LCE) < 25°
	Pistol grip deformity
	Coxa profunda
	120° < Neck shaft angle < 140°
	Acetabular retroversion
	Protrusio acetabuli
CT measurements	α angle > 50°
	Femoral retrotorsion

interobserver reliability with a minimum intraclass correlation coefficient of 0.88 for angle detection of the different motions.[11]

One observer (MKL) analyzed ROM for all patients in both groups with the software. Internal rotation was studied in 5° increments between 70° and 110° flexion and in 10° increments between –20° to 20° adduction. These ranges corresponded to the motion patterns evaluated in a conventional manual examination. For each of these patterns, the value of maximum impingement-free motion was computed for both groups and the three subgroups. We quantified the position of each impingement point of every possible combination of patterns detected on the acetabular rim, resulting in approximately 2000 to 4000 impingement points per patient. The distribution of the zones was virtually documented using the clock system.

The effect of surgical treatment on internal rotation was simulated for acetabular rim trimming and femoral offset creation only and for a combined treatment. The depth value for acetabular rim trimming was constant with a maximum resection depth of 3 mm. The extension of the virtually resected acetabular segment was chosen individually according to the impingement zone. After manual determination of the extension of the segment according to the clock system (Fig 3, points A and B), the computer automatically calculates the resection depth, which can be entered by the user. The radial cut is finally performed manually. In cam hips, the goal was to achieve a spherical head contour with a maximum alpha angle of 50°. This is accomplished by manual reshaping of the femoral head–neck junction with a virtual circle overlaying the patient's femoral head. The resulting ROM was compared between the study groups and among the three impingement subgroups before and after treatment.

We used the Kolmogorov-Smirnov test to determine normal distributions and paired and unpaired t tests to analyze normally distributed data. The Wilcoxon rank sum and Mann-Whitney U tests were used to compare paired and unpaired data without normal distribution. Fisher's exact test was used to assess associations between categorical variables. Differences among the three impingement subgroups were analyzed with the Kruskal-Wallis test. Significance was set at $p < 0.05$.

RESULTS

Hips with femoroacetabular impingement had decreased flexion ($p < 0.001$), internal rotation in 90° flexion ($p < 0.001$), and abduction ($p < 0.001$) compared with the control group (Table 2). There were no differences in adduction ($p = 0.927$), external rotation ($p = 0.194$), or extension (0.751). The impingement-free combined ROM was less ($p < 0.001$) for the femoroacetabular impingement group compared with the control group for each calculated pair of motions (flexion, internal rotation, and adduction/adduction) (Fig 4). Internal rotation decreased ($p < 0.001$) for both groups with increased flexion (Fig 4). Accordingly, increasing adduction to the flexed femur led to decreased ($p < 0.001$) internal rotation in both groups (Fig 4).

The impingement zones were localized in the anterosuperior quadrant of the acetabulum for the control and the impingement groups and did not differ when comparing the control with the femoroacetabular impingement group ($p = 0.366$) (Fig 5A). The average of the impingement locations was at 1.8 o'clock (standard deviation ± 1.8 hours) for the control group and at 1.9 o'clock (standard deviation ± 2.1 hours) in the femoroacetabular impingement group. Among the three impingement subgroups, the average of the impingement zone was similar in the three groups: at 1.7 o'clock (standard deviation ± 2.4 hours) in the cam, at 2.4 o'clock (standard deviation ± 2.4 hours) in the pincer, and at 1.7 o'clock (standard deviation ± 1.5 hours) in the combined subgroup (Fig 5B).

The virtual surgical resection of the impinging osseous prominences led to an increase of flexion ($p < 0.001$), internal rotation in 90° flexion ($p = 0.01$), and abduction ($p = 0.02$) (Table 2) and for all possible pairs of combinations with the various degrees of adduction for the study group ($p < 0.001$). In contrast, extension ($p = 0.051$), adduction ($p = 0.262$), and external rotation in 90° flexion ($p = 0.327$) were not affected by reshaping the joint (Table 2). As a result of virtual surgical reconstruction, internal rotation approached the reference curve of the normal group for the various degrees of flexion for all three subgroups (Fig 6). The average improvement of internal rotation for pincer hips after rim trimming was 5.4°. For cam hips, internal rotation increased by 8.5° after vir-

TABLE 2. Ranges of Motion of the Control (n = 33) and Study Groups (n = 28)

Parameter	Normal Hips	Femoroacetabular Impingement (preoperative)	p Value*	Femoroacetabular Impingement (after reshaping)	p Value†
Flexion	122° ± 16.3° (103°–145°)	105.2° ± 12.2° (69°–142°)	< 0.001	125.4° ± 9.7° (104°–143°)	< 0.001
Extension	56.5° ± 20.1° (12°–101°)	61.1° ± 31.8° (15°–129°)	0.751	71.1° ± 26.4° (16°–125°)	0.051
Abduction	63.3° ± 10.9° (40°–85°)	51.7° ± 12.2° (13°–71°)	< 0.001	63.6° ± 7.5° (50°–76°)	0.001
Adduction	32.7° ± 12.3° (4°–52°)	34.6° ± 12.3° (17°–64°)	0.927	35.8° ± 15.3° (17°–63°)	0.262
Internal rotation in 90° flexion	35.2° ± 6.9° (11°–61°)	11.1° ± 6.9° (0°–29°)	< 0.001	35.8° ± 15.3° (17°–63°)	0.002
External rotation in 90° flexion	102.5° ± 14.2° (75°–131°)	83° ± 33.7° (1°–126°)	0.194	93.9° ± 32.7° (27°–13°)	0.327

*Difference between normal hips and preoperative femoroacetabular impingement hips; †difference between preoperative value and after virtual reshaping

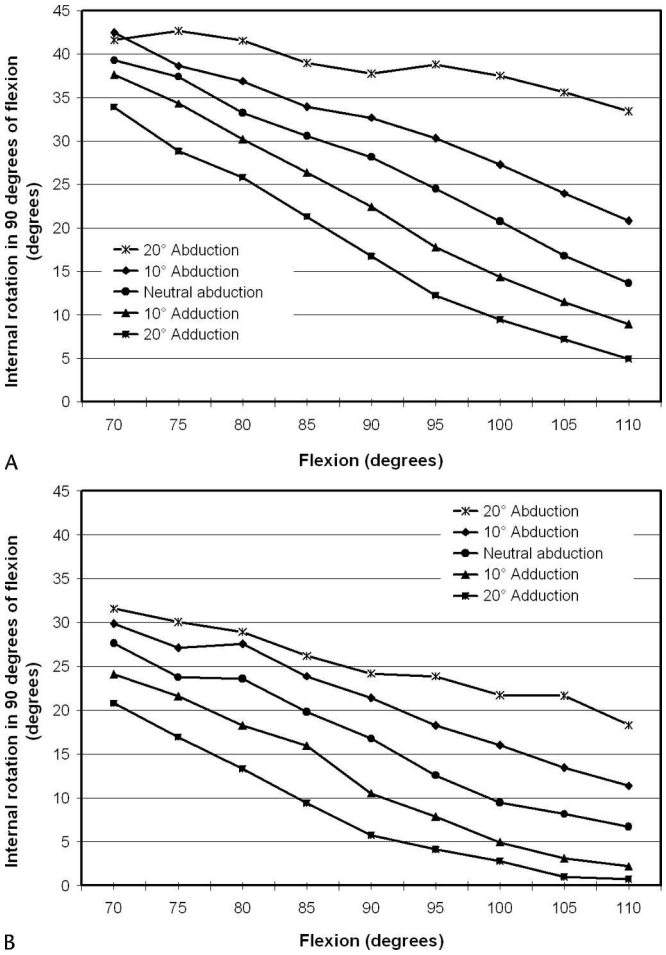

Fig 4A–B. (A) A graph shows the ROM pattern of the normal group. (B) The ranges were lower in the impingement group.

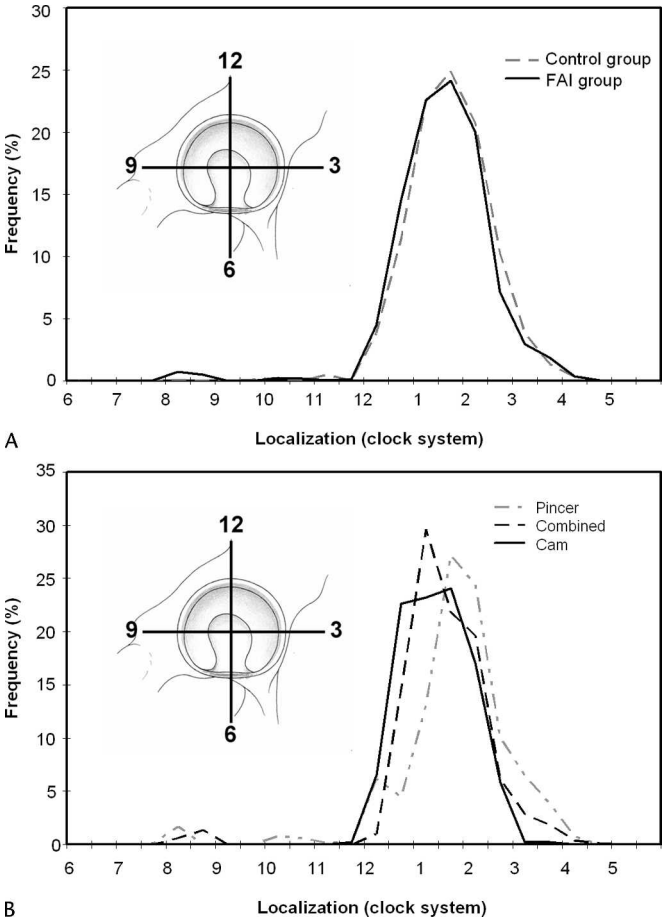

Fig 5A–B. (A) A similar distribution of impingement zones between the normal and the impingement groups is shown. Both were localized in the anterosuperior quadrant of the acetabulum. (B) There were no differences among the three different impingement groups.

tual femoral head reshaping. In the femoroacetabular impingement joints with combined impingement, this value reached 15.7° (10.6° of improvement after acetabular rim trimming and 5.5° after femoral head reshaping).

DISCUSSION

The 10-year THA failure rates in patients younger than 50 years are substantially higher than in elderly patients.[1] Joint-preserving surgery with the aim of avoiding or delaying additional degeneration is an attractive alternative. To date, in addition to classic osteotomies for acetabular dysplasia, surgical reconstruction of the hip for femoroacetabular impingement has been described and evaluated.[12,16] The underlying structural abnormalities in femoroacetabular impingement can be identified on conventional plain radiographs or 2-D MRI with intraarticular gadolinium contrast agent (arthro-MRIs).[6,9,12,14] However, although standard static 3-D rendering methods based on CT scans have been reported,[2] there is no interactive tool for dynamic investigation and 3-D visualization of anatomically based determination of the hip ROM and surgical planning for femoroacetabular impingement. Clinical measurement of hip ROM is subject to substantial error as a result of individual pelvic tilt and rotation.

In our computerized simulation, we did not include soft tissue tension as a limiting factor. Because the computer-generated analysis is limited to bone–bone impingement, the analyzed movements can exceed the real values because structures such as cartilage and labrum were not simulated. However, in the case of anterior femoroacetabular impingement with the relevant motions internal rotation and flexion, motion is restricted intraoperatively by bony contact.[6] The software can only provide calculations for concentric hips. If there is advanced osteoarthri-

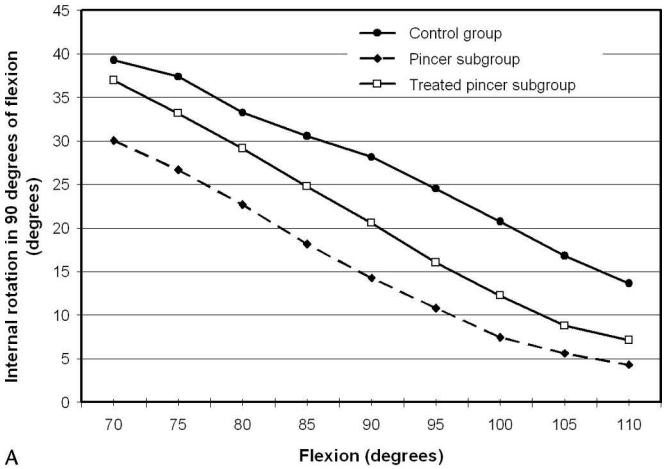

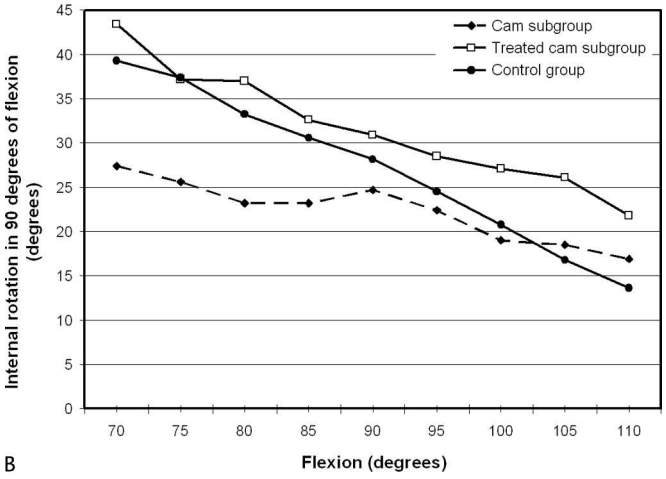

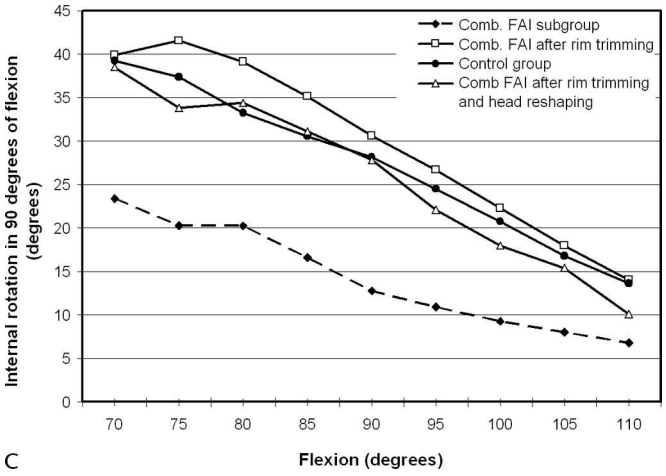

Fig 6A–C. (A) A graph shows the effect of rim trimming on the resulting ROM in hips with pincer impingement. The depth of the virtually resected acetabular segment was constant (3 mm). (B) A graph shows the effect of reconstructing a normal femoral head–neck offset in hips with cam impingement. The goal of the virtual reshaping was to create an alpha angle of 50°. (C) The effect of virtual reshaping in hips with combined femoroacetabular impingement is shown.

tis, the hip center moves and resulting motion consists not only of a rotation, but also of an additional translation, which cannot be simulated by our approach. Because advanced osteoarthritis with joint space narrowing is a relative contraindication for femoroacetabular impingement surgery, this limitation does not jeopardize the approach. Although a reproducibility and reliability study on calculating the ROM with our software has been published,[21] we have not performed an additional intraobserver or interobserver study on virtual reconstruction of the acetabulum and/or the femoral head–neck junction.

We present the developed software as a useful instrument for orthopaedic surgeons to noninvasively analyze preoperative impingement disorders. Hips with femoroacetabular impingement had reduced internal rotation with different degrees of abduction or adduction when referring to anatomic-based coordinate systems. Internal rotation decreased with increasing adduction in normal and impinging hips. The computer-detected impingement location on the acetabular rim in the femoroacetabular impingement group had almost identical distribution as in the control group. The only difference consisted of the earlier contact in the impingement group. This distribution matches the reported location of labral and chondral lesions in anterior femoroacetabular impingement, supporting the theory that joint damage in femoroacetabular impingement occurs at the impingement site.[3,19] As a general rule for clinical routine use, our data suggest eliminating the femoral source of impingement results in an improvement of 8° internal rotation, and a 3-mm surgical trimming of the acetabular rim increases the internal rotation by approximately 5°.

Several authors report computer-based impingement detection of the hip for similar indications.[10,18] Richolt et al described a method for impingement simulation in hips with slipped capital femoral epiphyses.[18] Kang et al described a similar joint simulation for hips with femoroacetabular impingement based on MRI.[10] In contrast to our approach, which assumed a fixed rotation center, these studies used a computer algorithm to increase the impingement-free motion by changing the rotation center.[10,18] If an unphysiologic impingement was detected, the virtual model of the femur was translated until it no longer collided with the pelvis assuring a more or less constant joint space width. Although such an approach may be feasible for obvious joint abnormalities (eg, slipped capital femoral epiphysis), it potentially can result in errors of ROM calculation in hips with slight deformities (eg, in a cam-type joint abnormality) because the aspheric portion of the femoral head could be underestimated. Unfortunately, none of these authors reported validation studies. Our approach with a fixed rotational center (the femoral head

TABLE 3. Comparison of Clinical Studies on Hip Range of Motion in Femoroacetabular Impingement

Authors, Year	Type of Measurement	Number	Type of Impingement	Treatment	Preoperative Flexion	Postoperative Flexion	Preoperative Internal Rotation	Postoperative Internal Rotation
Eijer et al, 2001[5]	Clinical	9	Cam (posttraumatic)	Bumpectomy through surgical hip dislocation	92° (80°–120°), no standard deviation documented	Increase by 11°	7° (−10°–20°), no standard deviation documented	Increase by 9°
Siebenrock et al, 2003[19]	Clinical	29	Pincer	Periacetabular osteotomy	99° (90°–110°), no standard deviation documented	106° (90°–120°)	11° (0°–30°), no standard deviation documented	21° (0°–40°), no standard deviation documented
Leunig et al, 2004[13]	Clinical	14	Not specified	Surgical hip dislocation	101° ± 16°, no range documented	No information	15° ± 12°, no range documented	No information
Jäger et al, 2004[9]	Clinical	17	Cam	Bumpectomy through surgical hip dislocation	108.4°, no standard deviation and range documented	108.9°, no standard deviation and range documented	8°, no standard deviation and range documented	21.7°, no standard deviation and range documented
Strehl & Ganz, 2005[20]	Clinical	11	Cam (posttraumatic)	Bumpectomy through surgical hip dislocation	95° (85°–120°), no standard deviation documented	100° (90°–120°), no standard deviation documented	15° (10°–45°), no standard deviation documented	20° (5°–30°), no standard deviation documented
Wettstein et al, 2006[23]	Clinical	15	Mixed, predominantly cam	Arthroscopy	108° ± 13°, no range documented	No detailed information	7° ± 12°, no range documented	No information
Present study	CT-based, computer-assisted	28	Cam, pincer, and combined	Virtual joint reconstruction	105.2° ± 12.2° (69°–142°)	125.4° ± 9.7° (104°–143°)	11.1° ± 6.9° (0°–29°)	35.8° ± 15.3° (17°–63°)

center) and tracked acetabular rim could be a fast and accurate method.

Our computerized analysis matches well with previously reported clinical data on ROM of hip impingement,[5,9,13,19,20,23] (Table 3) emphasizing the potential of this noninvasive method for routine clinical use. However, we have not confirmed any correlation between clinical and anatomically based virtual measurement of hip ROM.

It would be desirable to use routinely performed arthro-MRIs[14] for 3-D simulation of impingement instead of the CT used in this study. Additional radiation exposure and costs for the patient could be reduced. In addition, important soft tissue structures like labral and chondral lesions could be correlated directly with the location of impingement. However, segmentation based on MRI is difficult because it must be performed manually and is more time-consuming than established semiautomatic segmentation techniques based on CT. The restricted field of view is also limited to the hip. Important anatomic landmarks (particularly the distal femoral or the contralateral pelvic reference points) cannot be digitized in the data volume.

This computer-assisted noninvasive method is a novel approach to pathoanatomic mechanical hip problems. It may help the surgeon quantify the severity of impingement and provide guidance in choosing the appropriate treatment option. Because femoroacetabular impingement is not yet familiar to patients, and some may be unfamiliar with their hip disorders, a more logical observation of the pathomorphologic features will improve their understanding. In addition, clinical validation of our method is necessary to support its use. This approach is the basis for future techniques in which navigated instruments will allow intraoperative execution of previously planned osteoplasties. This could be combined with less invasive techniques such as hip arthroscopy[23] or techniques using smaller incisions without full surgical dislocation of the hip.

Acknowledgment

We thank Dr. Timo M. Ecker for contributions to this project.

References

1. Beaulé PE, Dorey FJ. Survivorship analysis of cementless total hip arthroplasty in younger patients. *J Bone Joint Surg Am*. 2001;83: 1590–1591.
2. Beaulé PE, Zaragoza E, Motamedi K, Copelan N, Dorey FJ. Three-dimensional computed tomography of the hip in the assessment of femoroacetabular impingement. *J Orthop Res*. 2005;23:1286–1292.
3. Beck M, Kalhor M, Leunig M, Ganz R. Hip morphology influences the pattern of damage to the acetabular cartilage: femoroacetabular impingement as a cause of early osteoarthritis of the hip. *J Bone Joint Surg Br*. 2005;87:1012–1018.
4. DiGioia AM, Jaramaz B, Blackwell M, Simon DA, Morgan F, Moody JE, Nikou C, Colgan BD, Aston CA, Labarca RS, Kischell E, Kanade T. The Otto Aufranc Award: image guided navigation system to measure intraoperatively acetabular implant alignment. *Clin Orthop Relat Res*. 1998;355:8–22.

5. Eijer H, Myers SR, Ganz R. Anterior femoroacetabular impingement after femoral neck fractures. *J Orthop Trauma*. 2001;15: 475–481.
6. Ganz R, Parvizi J, Beck M, Leunig M, Nötzli H, Siebenrock KA. Femoroacetabular impingement: a cause for osteoarthritis of the hip. *Clin Orthop Relat Res*. 2003;417:112–120.
7. Greene WB. The hip. In: Greene WB, Heckman JD, eds. *The Clinical Measurement of Joint Motion*. Rosemont, IL: American Academy of Orthopaedic Surgeons; 1994:99–114.
8. Hu Q, Langlotz U, Lawrence J, Langlotz F, Nolte LP. A fast impingement algorithm for computer-aided orthopedic surgery. *Comput Aided Surg*. 2001;6:104–110.
9. Jäger M, Wild A, Westhoff B, Krauspe R. Femoroacetabular impingement caused by a femoral osseous head–neck bump deformity: clinical, radiological, and experimental results. *J Orthop Sci*. 2004; 9:256–263.
10. Kang M, Sadri H, Moccozet L, Magnenat-Thalmann N, Hoffmeyer P. Accurate simulation of hip joint range of motion. *Proceedings of IEEE Computer Animation.* 2002;215–219.
11. Kubiak-Langer M, Tannast M, Murphy SB, Siebenrock KA, Langlotz F. Reliability study of the CT based system for range of motion calculation within the native hip joint. In: Langlotz F, Davies BL, Schlenzka D, eds. *Computer Assisted Orthopaedic Surgery*. 1st ed. Berlin, Germany: ProBusiness; 2005:261–263.
12. Lavigne M, Parvizi J, Beck M, Siebenrock KA, Ganz R, Leunig M. Anterior femoroacetabular impingement. Part I: techniques of joint preserving surgery. *Clin Orthop Relat Res*. 2004;418:61–66.
13. Leunig M, Podeszwa D, Beck M, Werlen S, Ganz R. Magnetic resonance arthrography of labral disorders in hips with dysplasia and impingement. *Clin Orthop Relat Res*. 2004;418:74–80.
14. Locher S, Werlen S, Leunig M, Ganz R. MR-arthrography with radial sequences for visualization of early hip pathology visible on plain radiographs [in German]. *Z Orthop Ihre Grenzgeb*. 2002;140: 52–57.
15. Murphy SB, Simon SR, Kijewski PK, Wilkinson RH, Griscom T. Femoral anteversion. *J Bone Joint Surg Am*. 1987;69:1169–1176.
16. Murphy SB, Tannast M, Kim YJ, Buly R, Millis MB. Debridement of the adult hip for femoroacetabular impingement: indications and preliminary clinical results. *Clin Orthop Relat Res*. 2004;429: 178–181.
17. Nötzli HP, Wyss TF, Stöcklin CH, Schmid MR, Treiber K, Hodler J. The contour of the femoral head–neck junction as a predictor for the risk of anterior impingement. *J Bone Joint Surg Br*. 2002;84: 556–560.
18. Richolt JA, Teschner M, Everett PC, Millis MB, Kikinis R. Impingement simulation of the hip in SCFE using 3D models. *Comput Aided Surg*. 1999;4:144–151.
19. Siebenrock KA, Schöniger R, Ganz R. Anterior femoro-acetabular impingement due to acetabular retroversion: treatment with periacetabular osteotomy. *J Bone Joint Surg Am*. 2003;85:278–286.
20. Strehl A, Ganz R. Anterior femoroacetabular impingement after healed femoral neck fractures. *Unfallchirurg*. 2005;108:263–273.
21. Tannast M, Kubiak-Langer M, Langlotz F, Puls M, Murphy SB, Siebenrock KA. Noninvasive three-dimensional assessment of femoroacetabular impingement. *J Orthop Res.* 2007;25:122–131.
22. Tannast M, Langlotz U, Siebenrock KA, Wiese M, Bernsmann K, Langlotz F. Anatomic referencing of cup orientation in total hip arthroplasty. *Clin Orthop Relat Res*. 2005;436:144–150.
23. Wettstein M, Dienst M. Hip arthroscopy for femoroacetabular impingement [in German]. *Orthopade*. 2006;35:85–93.